Improving the Shale Gas Production Data Using the Angular- Based Outlier Detector Machine Learning Algorithm

Taha Yehia[1,2*], Hamid Khattab[2], Mahmoud Tantawy[2], Ismail Mahgoub[1]

[1] *Department of Petroleum Engineering, Faculty of Engineering and Technology, Future University in Egypt (FUE), Cairo 11835, Egypt*

[2] *Department of Petroleum Engineering, Faculty of Petroleum and Mining Engineering, Suez University, Suez 11252, Egypt*

* Corresponding Author ORCID https://orcid.org/0000000154896701

Email Address: tahayehia52@gmail.com (Taha Yehia); hamidkhattab@hotmail.com (Hamid Khattab); mahmoud.tantawy@pme.suezuni.edu.eg (Mahmoud Tantawy) & ismail.shaaban@fue.edu.eg (*Ismail Mahgoub*)

Abstract

Production history is essential for any reservoir engineering study. It used for history matching in reservoir simulation study, rate transient analysis and decline curve analysis (DCA). The quality of the production data is important. Better quality of the production data reduces the uncertainties during modeling the reservoir, characterizing it and forecasting the future production.

Shale gas reservoirs have been developed heavily in last two decades. They have huge reserves but there are challenges in evaluating them economically. Transient flow that could last for long time, liquid loading causing successful shut ins and controlling the bottom hole flowing pressure cause the production data to fluctuate heavily. The noisy production profile makes it difficult to detect the different flow regimes precisely and affects analysis such DCA.

In this paper, we used a machine learning algorithm called angular- based outlier detector (ABOD) to improve the production data of 4 shale gas wells. It was assumed that 20% of the production data is noise and the algorithm is asked to determine the points with the highest potential to be detected as noise. After that, the different flow regimes were determined before and after improving the data quality.

The results show that the ABOD algorithm removed the noise from the production data efficiently. The production profile was smoothed without any bias and without removing any significant event. Detecting the different flow regimes was much clear after removing the noise. Moreover, we determined the masked flow regimes after improving the production data quality in some cases.

1. Introduction

Any piece of data can include information. It's critical to understand what kind of data is being analyzed. The study's desired results dictate the type of analysis conducted on the data. The effort, time, and cost of every study are crucial.

PVT data, core data, logs data, pressure transient data and production history data are such examples of the data types that used by the reservoir engineers. Analyzing these different kinds data introduces valuable understanding of the whole field and there for lead to better

planning the field, well spacing, characterizing the reservoir, determining the reserves, sizing the production facilities, deciding investing profile and more are based on the kind of the analyzing methods being used.

The major reservoir engineering data analysis methods are:

- Data driven empirical models
- Analytical or physics based models:
  - Pressure transient analysis (PTA)
  - Rate transient analysis (RTA)
- Numerical simulation models and recently;
- Machine learning (ML) models.

Analytical and numerical simulation methods require data such as fluid and rock properties, geological and construction parameters, production history and some assumptions. Using one of these models requires time and effort as modelling complex mechanisms is not easy at all. [1–4].

Material balance methods use the law of mass conservation and the remaining volumes of any reservoirs equal the total volume minus the produced volumes. Driving mechanism, water aquifers or gas caps and rock and fluid properties are considered in this method. Using the production data for such a study in shale gas reservoirs faces two problems:

- MB needs at least two stabilized reservoir pressure points. In shale gas, this is hard being achieved as the well may be in the transient flow for very long time.
- The driving mechanisms related to producing shale gas such as gas slippage, diffusion and desorption are hard to determine contribution of each to the production.

Empirical and advanced DCA are considered to be the easiest and fastest methods compared to analytical and numerical simulation ones. But since there are a lot of uncertainties related to the production data, there are uncertainties related to the calculated EUR. Based on that, probabilistic DCA is recommended. [5–7].

The common required data for all of this analyzing methods is the production history. Therefore, improving the production data before conduct and of these analysis is essential. The question is how to remove it efficiently without removing any data or trend within the production profile that has meaning.

In this paper, we used a machine learning algorithm called angular- based outlier detector (ABOD) to improve the production data of 4 shale gas wells. It was assumed that 20% of the production data is noise and the algorithm is asked to determine the points with the highest potential to be detected as noise. After that, the different flow regimes were determined before and after improving the data quality.

1.1. WHY SHALE GAS RESERVOIRS?

The demand on nature gas has greatly increased and will continue to grow in the next decades. Due to the global trend to reach net zero emissions of $Co_{2,}$ the natural gas is considered the backbone of the energy transition as it is a clean energy resource compared to other resources of fossil fuels. **Figure (1)** shows a forecasting of the gap between the production and the consumption will exist by 2050. Shale gas reservoirs have huge extended reserves. Continues developing of these reserves could help narrowing this gap in the future. **Figure (2)** shows the

forecasted incensement in production from shale gas reservoirs compared to conventional reservoirs.

1.2. Shale gas characteristics

The shale matrix's very small pores are a defining feature of shale gas reserves. These pores range in size from micro to nano size. [8] The shale matrix's porosity is less than 10%, and its permeability is extremely low (less than 10-8 Darcy). The bedding trend and the in-place pressures brought on by the compaction of shale both have an impact on the permeability of the rock. Permeability may only be 10(-8) Darcy. [9] Shale gas reservoirs may contain naturally fractures as a result of stresses matrix shrinkage. [10] Shale gas reserves contain enormous amounts of trapped gas, more than 94 percent of which is methane. This gas may exist in three different states: it may be free in the matrix and fractures, adsorbed by organic matter and clay minerals, or dissolved in asphaltenes and shale oil. [11] The free gas is the major source of production from shale gas resources. Comparatively, the adsorbed gas, which might make up 20 to 85% of the entire gas volume, is taken into account rather than the dissolved gas volume. These fluid and rock qualities result in complicated driving mechanisms that produce this gas. There are three basic mechanisms: desorption, diffusion, and slippage.

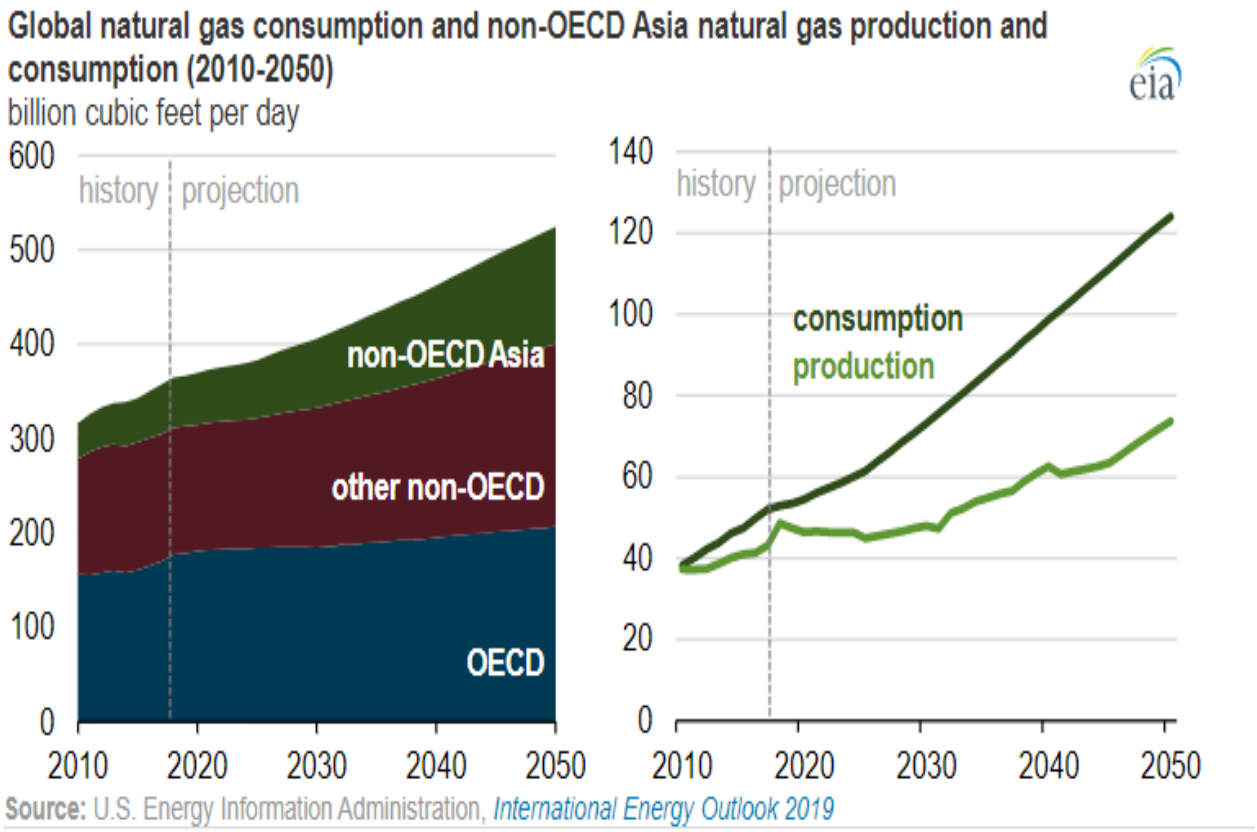

Figure 1. shows a forecasting of the gap between the production and the consumption will exist by 2050.

1.1. Challenges Related to Analyzing the Producing Shale Gas wells

Under natural conditions, producing from shale gas reservoirs with economic value is difficult. Drilling horizontal wells with several stages of hydraulic fracturing is the best way to create shale gas reserves. Blocks of stimulated reservoir volume are produced as a result, along with transverse or longitudinal fractures (SRV).

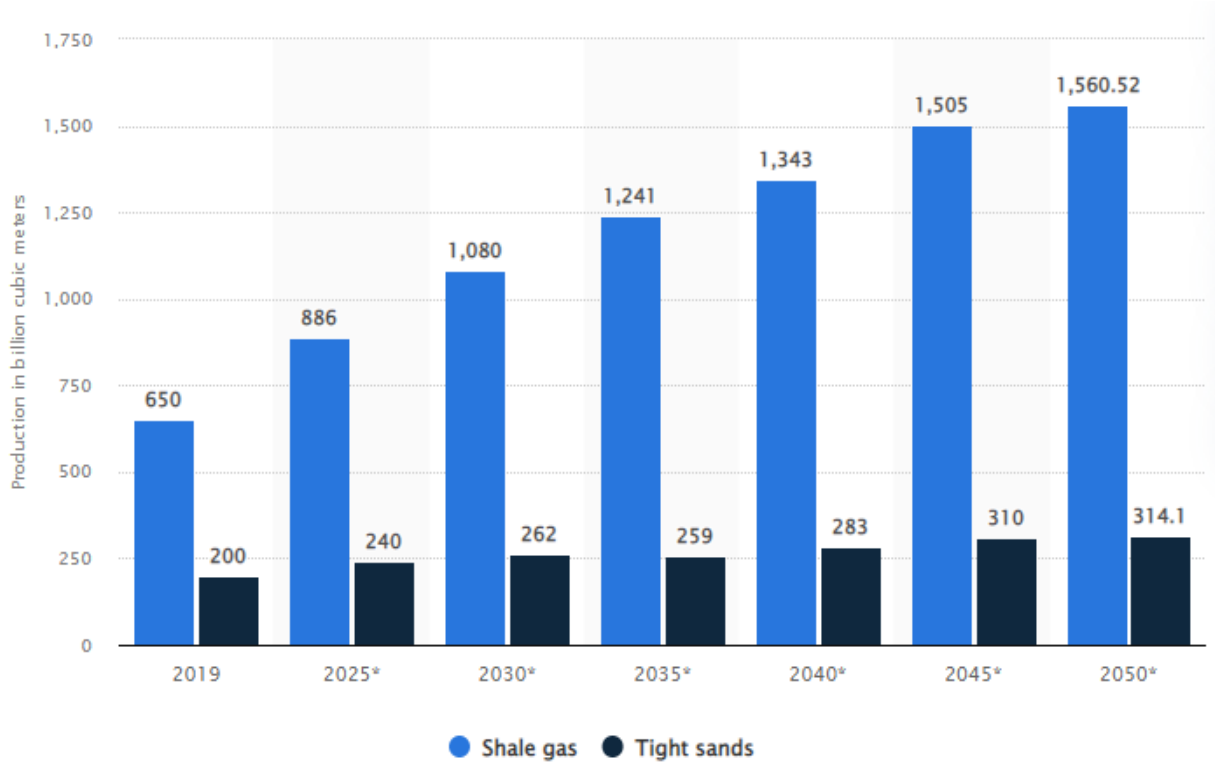

Figure 1. shows the forecasted production from shale gas reservoirs compared to conventional reservoirs.

The larger the SRV that might be created, the longer the well's horizontal length and the more stages it has. However, this method of production results in a complicated system with a network of interrelated natural fractures, hydraulic fractures, and a matrix with extremely poor permeability. Complex flow regime sequences are the actual result.

The following combinations of flow regimes may be present while developing shale gas wells and have an effect on the output decrease trends:[12–15]

- **Linear Flow:** It could have been the primary flow throughout the well's lifetime. From the matrix to the hydraulic fractures, it is perpendicular. Plotting the flow rate vs time on a Log-Log plot can help you find the transient linear flow. If there are no natural fractures in the reservoir, the map displays a -1/2 slope.
- **Linear–Boundary Dominated Flow (BDF)**: The BDF appears after a brief appearance of the transient linear. Usually, it has to do with getting to the SRV's bounds. This might be seen on a log-log plot as the slope starts to deviate from 1/2 slope starts to appears.
- **Bilinear–Linear:** In this scenario, bilinear flow is supposed to be the starting flow regime (linear followed by another linear). When it occurs and lasts for a relatively little time in

the beginning, it is typically associated to natural fractures. In this instance, the flow simultaneously travels linearly from the matrix to the fractures and from the fractures to the well. Accordingly, a -1/4 slope on a log-log plot indicates a bilinear flow, while a -1/2 slope indicates a linear flow.

- **Bilinear-linear-BDF:** When the flow approached the SRV borders and the Log-Log plot once more deviates from the -1/2 slope, this situation is distinct from the previous example.

Figure 3 demonstrates how the Log-Log plot is used to describe various flow regimes. It should be noted that whether or not the reservoir is naturally broken affects whether one of these scenarios appears. This also has to do with fracture conductivity**.**

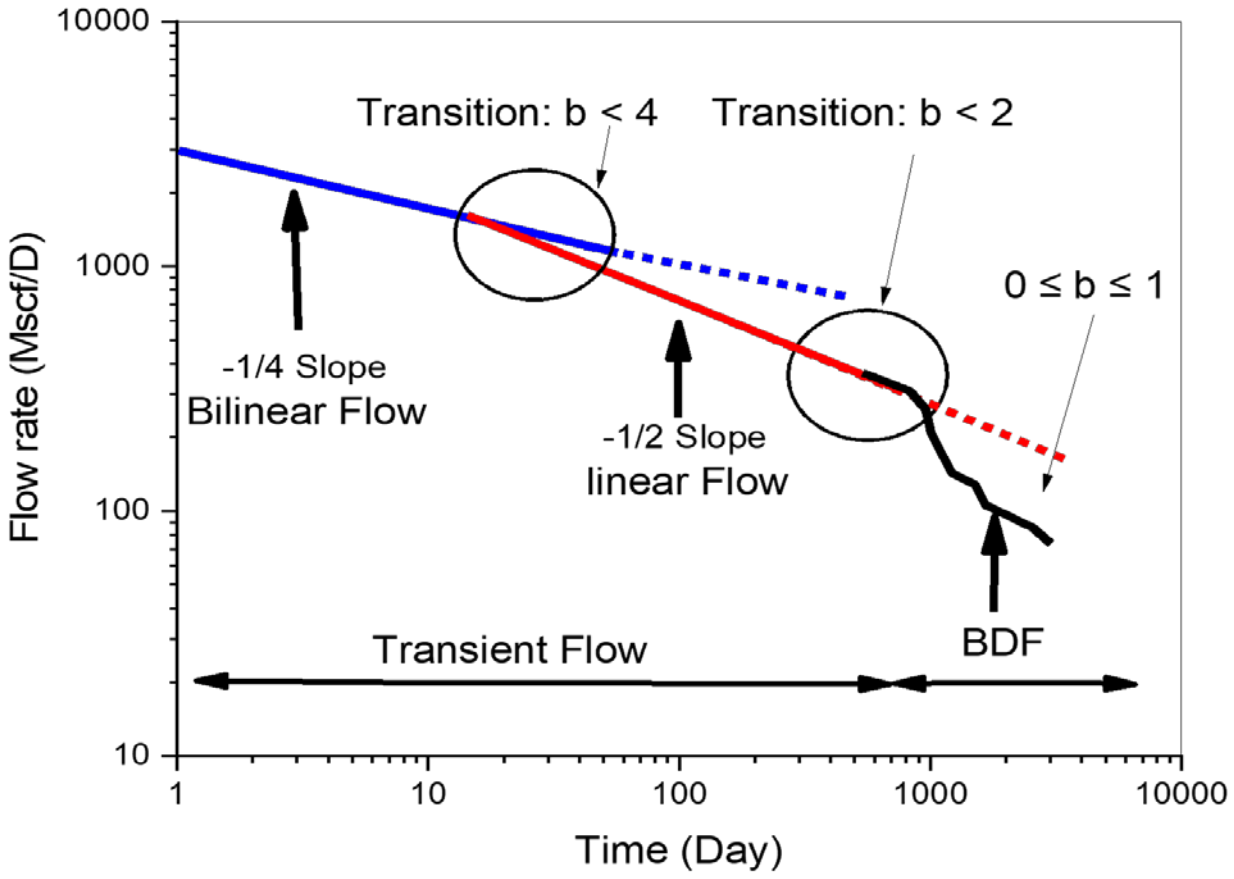

Figure 3. Identifying the different flow regimes based on the slope value on the log-log plots[14]**.**

Controlling the bottom hole pressure (BHP) during production is crucial for raising EUR. This reduces the stress impact, controls proppant backflow, and stops related water from building up in the wellbore. [16] Even if establishing SRV and managing BHP are crucial for the development of shale gas reservoirs and their appropriate implementation helps to improve the EUR, estimating the EUR itself is difficult as a result of these procedures. [17] Since the SRV is the primary source of flow during the early stages of production, the flow rate is high. [18] The flow transitions from transient flow to boundary dominated flow (BDF) when it approaches the

SRV's borders, generating a sharp decline in the flow rate profile before continuing with a long tail production profile. [3] However, modifying the BHP results in significant changes to the production data itself, and the noise level may be excessive. Therefore, it is difficult to adequately match the production data using decline curve models as a result of the results of these two practises. [19]

2. Removing the Outlier using ML Algorithm

After adding artificial noise to simulated data, Jha et al. tested the five well-known outlier identification approaches. The detectors that were looked into were isolation forest, distance-based outlier detection, density-based outlier detection, and angle-based outlier detection. [20]

Investigation led to the discovery that the ABOD is the most effective algorithm. Assuming that 20% of the data are noise, the ABOD algorithm was assigned to filter outlier and inlier data. The ABOD is to identify the highest 20 percent of the data that should be regarded as an outlier.

Figures 4 and 5 depict the operation of the ABOD algorithm. It begins by setting up the observation of interest's k nearest neighbours and computing the k vectors that extend from the observation to those neighbours. Equation 1 is used to compute the weighted scalar product of all possible pairings of different vectors that were found in the previous stage.

$$\left(\frac{\langle \bar{AB}.\bar{AC} \rangle}{\|\bar{AB}\|^2 \|\bar{AC}\|^2}\right), \quad (1)$$

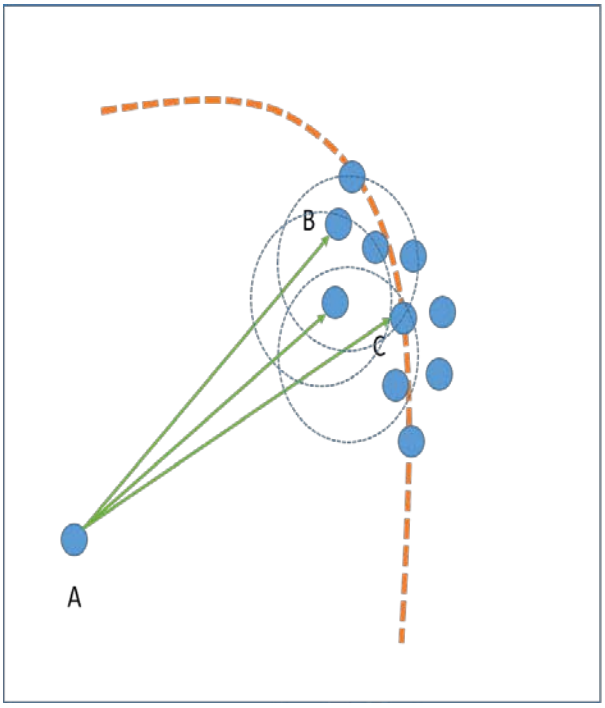

Figure 4. K[th] nearest neighbors for point A, k = 3.

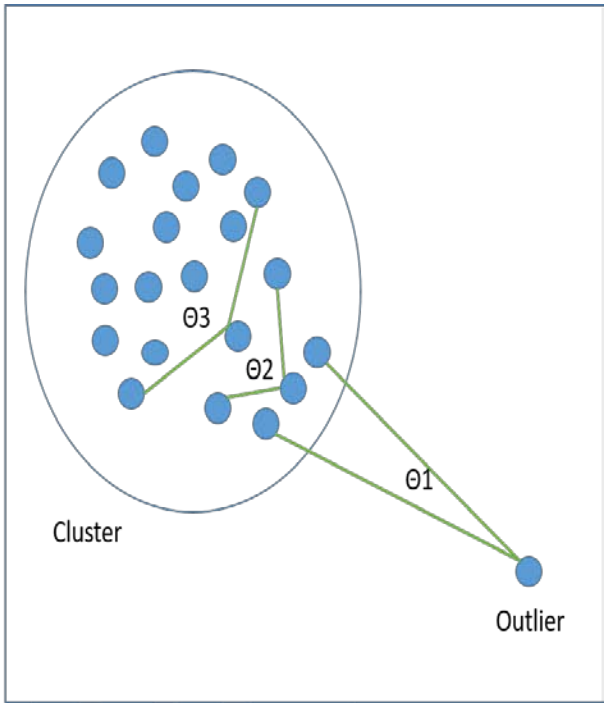

Figure 5. An outlier has low variance in its angle with other data points as compared to an inlier.

3. Data

The data used in this study is actual data. The data was released in 2021 on the SPE official website. The data repository has more than fifty wells between shale gas production and shale oil. 6 wells were selected. The production is mainly dry gas. The choice of this certain wells was based on having variety of production profile durations and different level of noise through the data to better clear the aim of this study. **Tables (1) through (4**) shows the characteristics of each well.

Table 1. Well_12

The Specifications of Well_12. [21]			
State	LA	**TVD (ft)**	11258.854
Formation/Reservoir	HAYNESVILLE SHALE	**Spacing**	-
Initial Pressure Estimate (psi)	9939	**Stages**	10
Reservoir Temperature (deg F)	285.21375	**Clusters**	69
Net Pay (ft)	268.39703	**Clusters per Stage**	7
Wellbore Diameter (ft)	0.7	**Lateral Length (ft)**	4496
Porosity	0.088000059	**Top Perf (ft)**	11253
Water Saturation	0.183792612	**Bottom Perf (ft)**	15749
Oil Saturation	0	**Sandface Temp (deg F)**	285.21375
Gas Saturation	0.816207388	**Static Wellhead Temp (deg F)**	120
Gas Specific Gravity	0.58	**Casing Depth (ft)**	15800
Condensate Gravity (API)	30	**Tubing OD (in)**	2.375
Dew Point Pressure (psi)	9893.27	**Tubing Depth (ft)**	11224.67
Sep. Temperature (deg F)	100	**Casing ID 1 (in)**	4.67
Sep. Pressure (psi)	100	**Casing Depth (ft)**	15800

Table 2. Well_24

The Specifications of Well_24. [22]			
State	LA	**TVD (ft)**	12064.16
Formation/Reservoir	HAYNESVILLE SHALE	**Spacing**	1050
Initial Pressure Estimate (psi)	10450	**Stages**	66
Reservoir Temperature (deg F)	329	**Clusters per Stage**	7
Net Pay (ft)	193	**Lateral Length (ft)**	9820
Wellbore Diameter (ft)	0.7	**Top Perf (ft)**	12470
Porosity	0.08612	**Bottom Perf (ft)**	22290
Water Saturation	0.21	**Sandface Temp (deg F)**	329
Oil Saturation	0	**Static Wellhead Temp (deg F)**	236
Gas Saturation	0.79	**Production Path**	Casing
Gas Specific Gravity	0.594	**Casing ID 1 (in)**	4.67

Condensate Gravity (API)	30	**Casing Footage 1 (ft)**	11421
Sep. Temperature (deg F)	100	**Casing ID 2 (in)**	4.28
Sep. Pressure (psi)	100	**Casing Footage 2 (ft)**	10885
Oil Gravity (API)	30	**Casing Depth (ft)**	22306
Clusters	462		

Table 3. Well_27

The Specifications of Well_27. [23]			
State	PA	**Bubble Point Pressure (psi)**	20000
Formation/Reservoir	MARCELLUS	**TVD (ft)**	5707.639
Initial Pressure (psi)	3486	**Stages**	13
Reservoir Temperature (deg F)	115	**Clusters**	65
Net Pay (ft)	101.6	**Clusters per Stage**	5
Wellbore Diameter (ft)	0.7	**Lateral Length (ft)**	5210
Porosity	0.070015	**Top Perf (ft)**	5900
Water Saturation	0.3297	**Bottom Perf (ft)**	11110
Oil Saturation	0.001304	**Sandface Temp (deg F)**	115
Gas Saturation	0.668996	**Static Wellhead Temp (deg F)**	65
Gas Specific Gravity	0.57	**Production Path**	Tubing
Condensate Gravity (API)	30	**Tubing ID (in)**	2.441
Dew Point Pressure (psi)	20000	**Tubing OD (in)**	2.875
Sep. Temperature (deg F)	100	**Tubing Depth (ft)**	5172
Sep. Pressure (psi)	100	**Casing ID 1 (in)**	4.778
Oil Gravity (API)	30	**Casing Footage 1 (ft)**	11238
Initial GOR (scf/bbl)	591.613	**Casing Depth (ft)**	11238

Table 4. Well_40

The Specifications of Well_40. [24]			
State	PA	**TVD (ft)**	6936.15
Formation/Reservoir	MARCELLUS - UPPER	**Spacing**	1500
Initial Pressure Estimate (psi)	3150	**Stages**	75
Reservoir Temperature (deg F)	124.56	**Clusters**	373
Net Pay (ft)	230.5	**Clusters per Stage**	4.973333333
Wellbore Diameter (ft)	0.7	**Lateral Length (ft)**	13011
Porosity	0.0675	**Top Perf (ft)**	6948
Water Saturation	0.27	**Bottom Perf (ft)**	19959
Oil Saturation	0	**Sandface Temp (deg F)**	125

Gas Saturation	0.73	**Static Wellhead Temp (deg F)**	60
Gas Specific Gravity	0.57	**Production Path**	Casing
Condensate Gravity (API)	30	**Casing ID 1 (in)**	4.778
Sep. Temperature (deg F)	100	**Casing Footage 1 (ft)**	20087.6
Sep. Pressure (psi)	100	**Casing Depth (ft)**	20087.6
Oil Gravity (API)	30		

4. Analysis

In this chapter, the impact of removing the outliers from the production data of the selected wells is shown using the ABOD algorithm. For each well, we will present the production profile before and after removing the outliers. Also, the different flow regimes are identified before and after removing the outliers.

4.1. WELL_12

Figures (1) and (2) show the actual production profile, and the production profile after removing 20% of the production data as noise and the removed noise of well_12 successfully.

Figures (3) and (4) show how the different flow regimes are identified from the log-log plot of the flow rate versus time by detecting the trend line with the characteristic slope of each one.

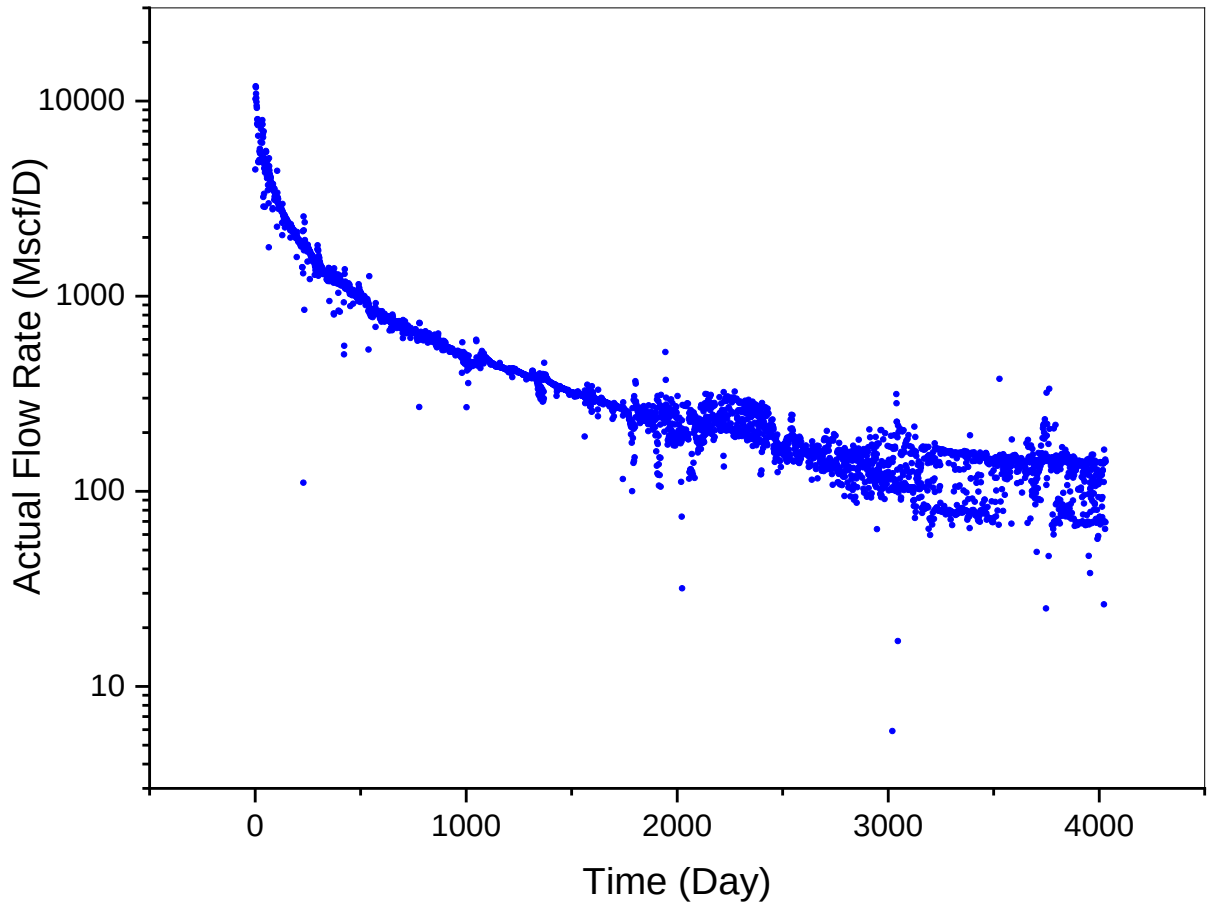

Figure 2. The actual production data before removing outlier.

ABOD removes the isolated points. After that, it removes closer by closer points without masking any trends within the production profile.

Figure (3) shows the log-log plot of the actual flow rate versus time before removing the outliers while **Figure (4)** shows the same plot but after removing 20% from the production data as noise successfully.

The removed noise takes the same profile of the production data. This means that the noise was not concentrated in a specific period. Although the slopes of the trend lines related to the linear and pseudo steady state flow regimes are clear to be identified before the removing any noise but removing the noise helped smoothing the trends and became clearer.

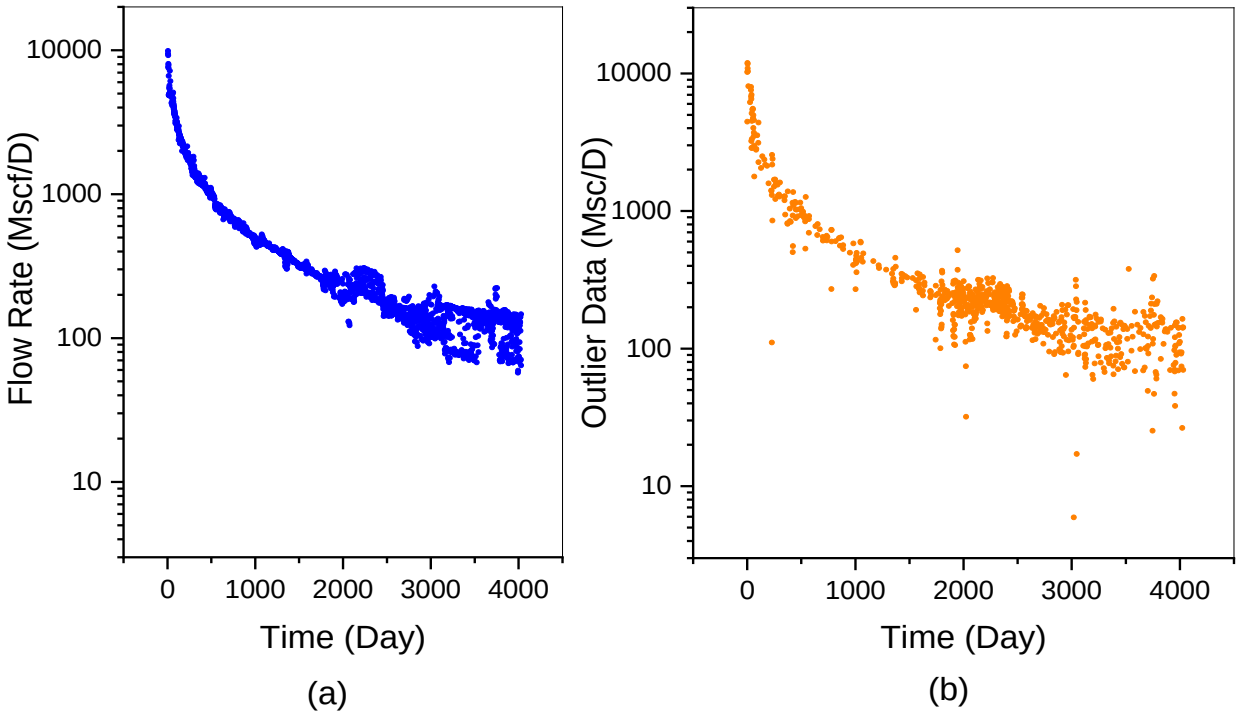

Figure 2. (a) The production data after removing 20% as outlier. (b) The removed data.

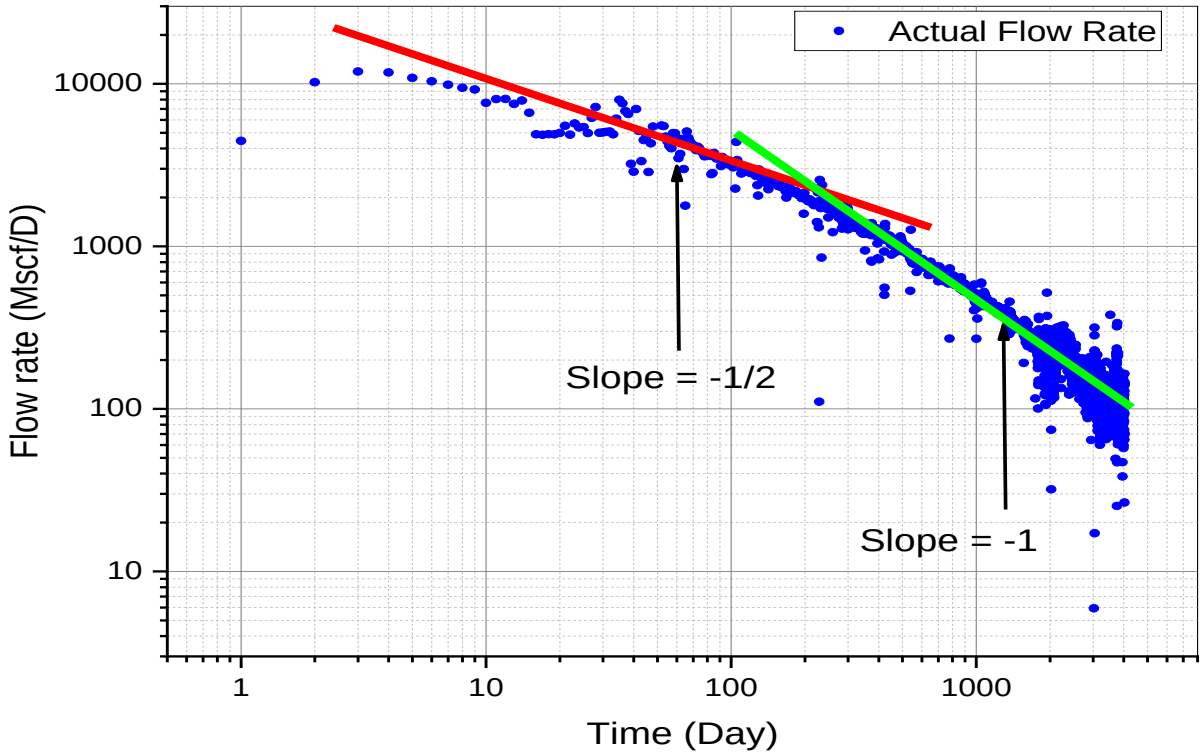

Figure 3. Shows identifying the flow regimes before removing the noise.

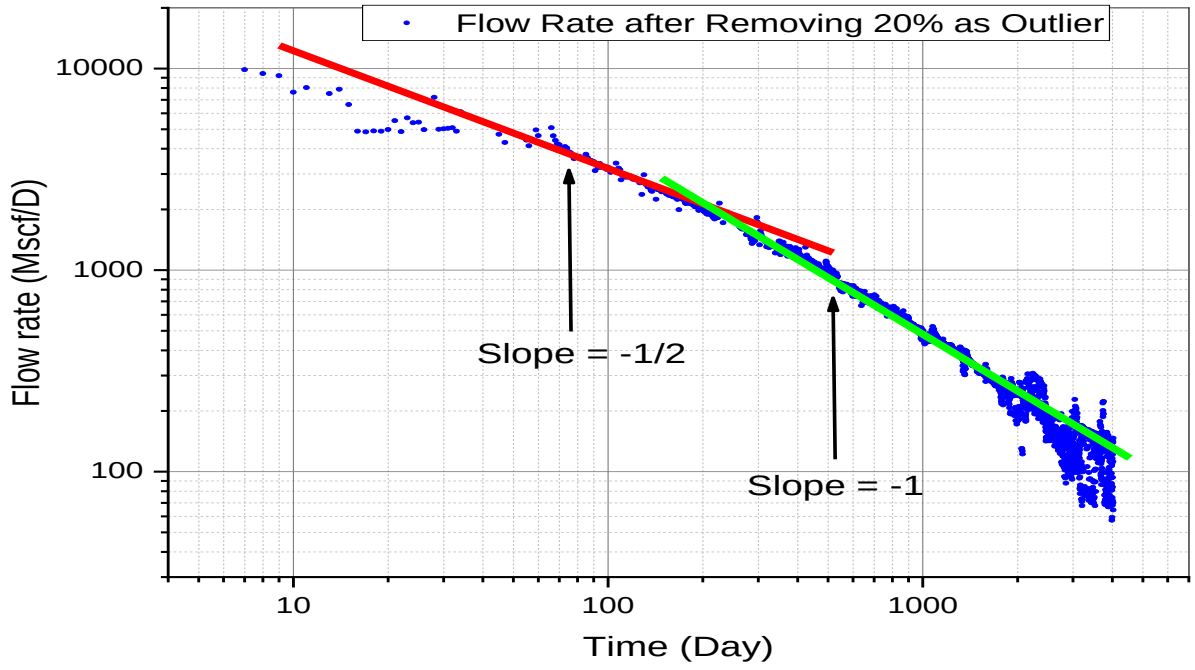

Figure 4. Shows identifying the flow regimes after removing 20% as the noise.

4.2. WELL_24

Figures (5) and (6) show the actual production profile and the production profile after removing 20% of the production data as noise and the removed noise of well_24 successfully.

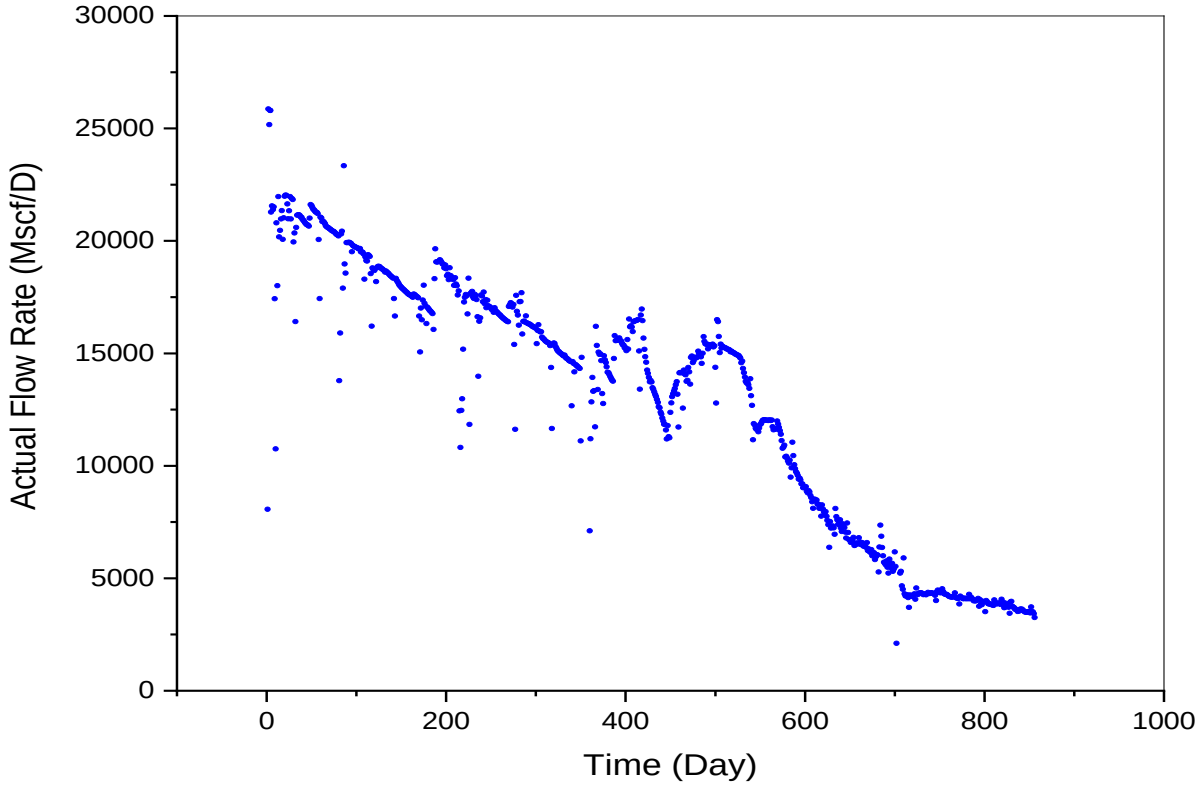

Figure 5. The actual production data before removing outlier.

Figures (7) and (8) show how the different flow regimes are identified from the log-log plot of the flow rate versus time by detecting the trend line with the characteristic slope of each one.

Looking at the production profile of this well, we could notice that most of the noise are concentrated in the early time of the production while the late time is much smoother.

The removed noise is not equally through the production profile. The ABOD algorithm removed more noise point from the early time which is noisier than the late time. This is one of the advantages of the ABOD algorithm. At the beginning, it removes the isolated points. After that, it removes closer by closer points without masking any trends within the production profile.

Figure (7) shows the log-log plot of the actual flow rate versus time before removing the outliers while **Figure (8)** shows the same plot but after removing 20% from the production data as noise .

Before removing the noise, we identified two trend lines related to the linear and BDF flow as shown in **Figure (7).** After removing the noise, we identified three trend lines related to the bilinear, linear, and BDF as shown in **Figure (8)**. Because most of the removed noise was from the early time of the production, we differentiated between the bilinear and linear flow regime clearly after removing the noise.

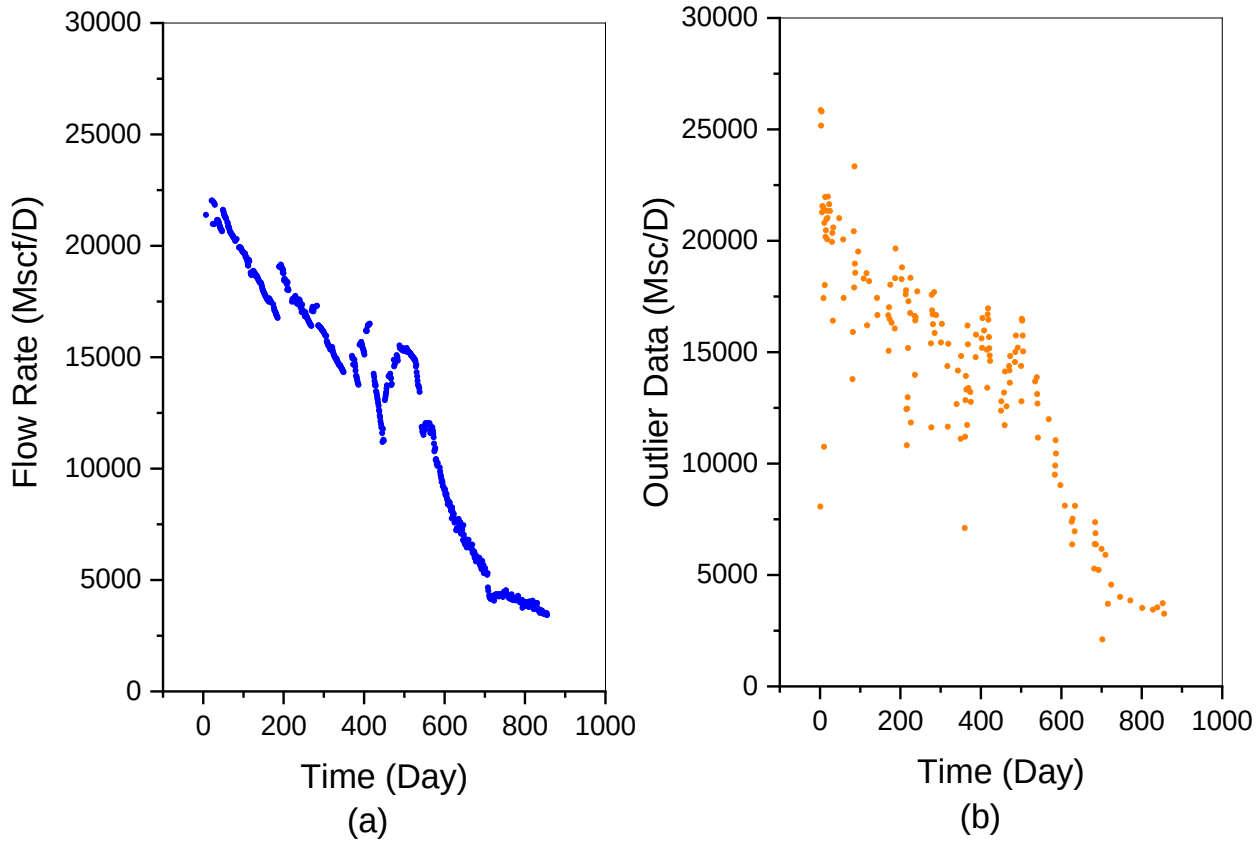

Figure 6. (a) The production data after removing 20% as outlier. (b) The removed data.

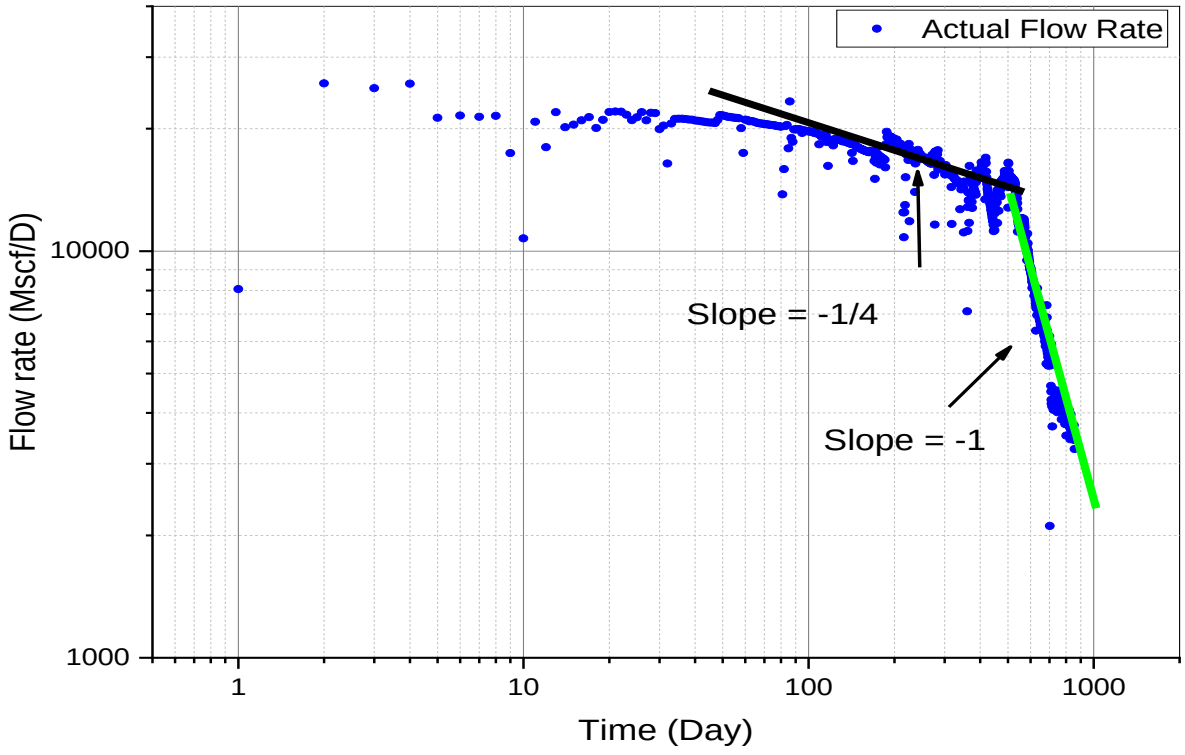

Figure 7. Shows identifying the flow regimes before removing the noise.

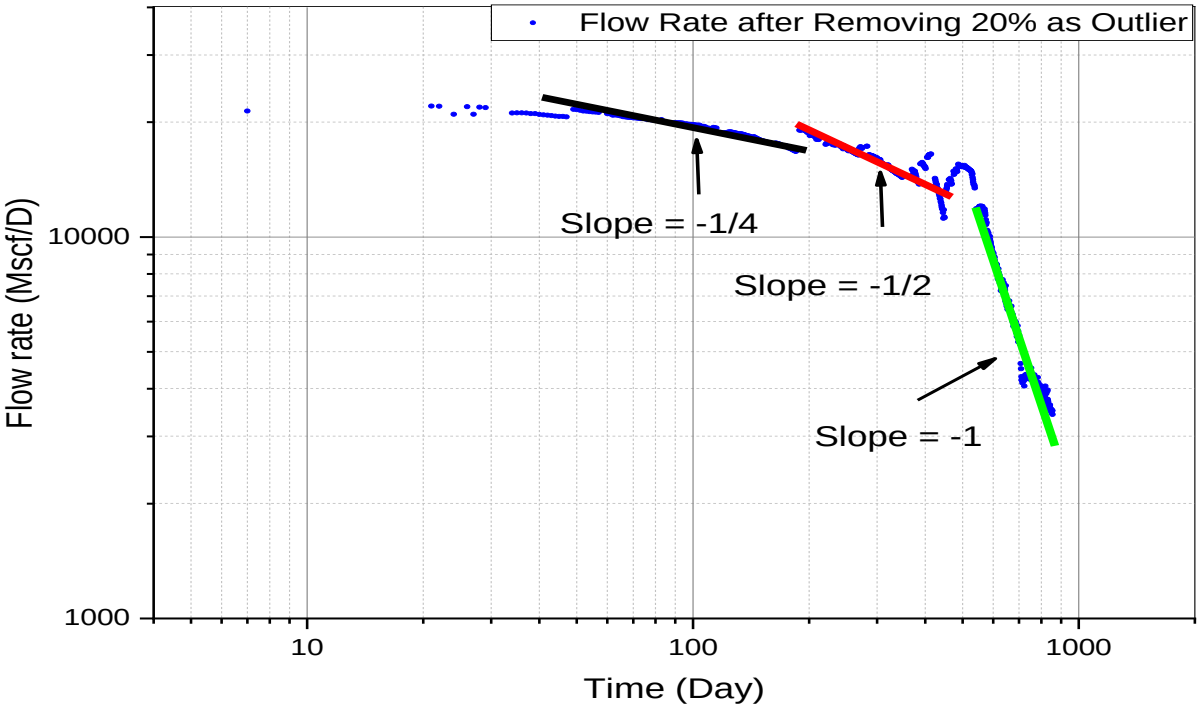

Figure 8. Shows identifying the flow regimes after removing 20% as the noise.

4.3. WELL_27

Figures (4.9) and (10) show the actual production profile, the production profile after removing 20% of the production data as noise and the removed noise of well_27 successfully.

Figures (4.11) and (4.12) show how the different flow regimes are identified from the log-log plot of the flow rate versus time by detecting the trend line with the characteristic slope of each one.

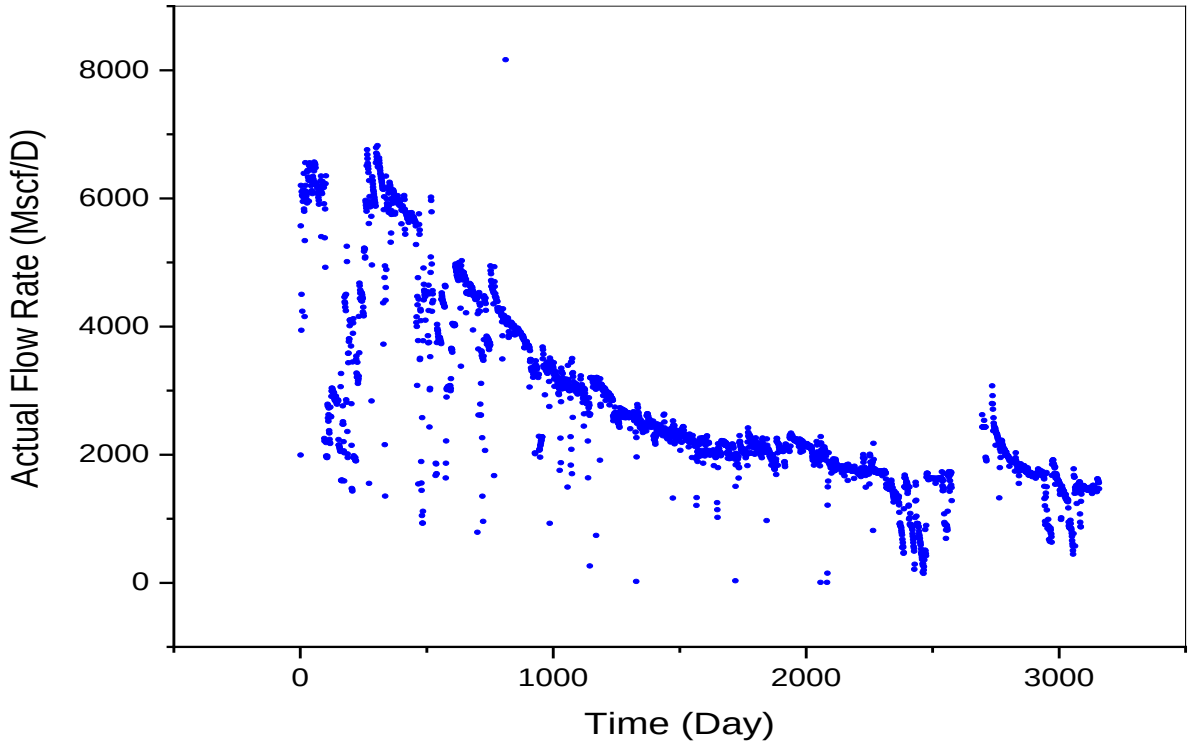

Figure 9. The actual production data before removing outlier.

Looking at the production profile of this well, we could notice that it is too noisy especially at the early time of the production. This was because of the flow back of the fracturing fluids and controlling the BHP by changing the chock size continuously. In late time, there is fluctuations in the production profile too. This was because of liquid loading caused successful shut ins.

The removed noise is scattered through all the production profile. The ABOD algorithm removed more noise point from the early time which is noisier than the late time. At the beginning, it removes the isolated points. After that, it removes closer by closer points without masking any trends within the production profile.

Figure (4.11) shows the log-log plot of the actual flow rate versus time before removing the outliers while **Figure (4.12)** shows the same plot but after removing 20% from the production data as noise.

Before removing the noise, we identified one trend line related to the linear flow as shown in **Figure (4.11).** After removing the noise, we identified two trend lines related to the bilinear and linear as shown in **Figure (4.12).** Because the removed noise was scattered along the production profile, the period of the linear flow lasted for shorter time than before removing the noise.

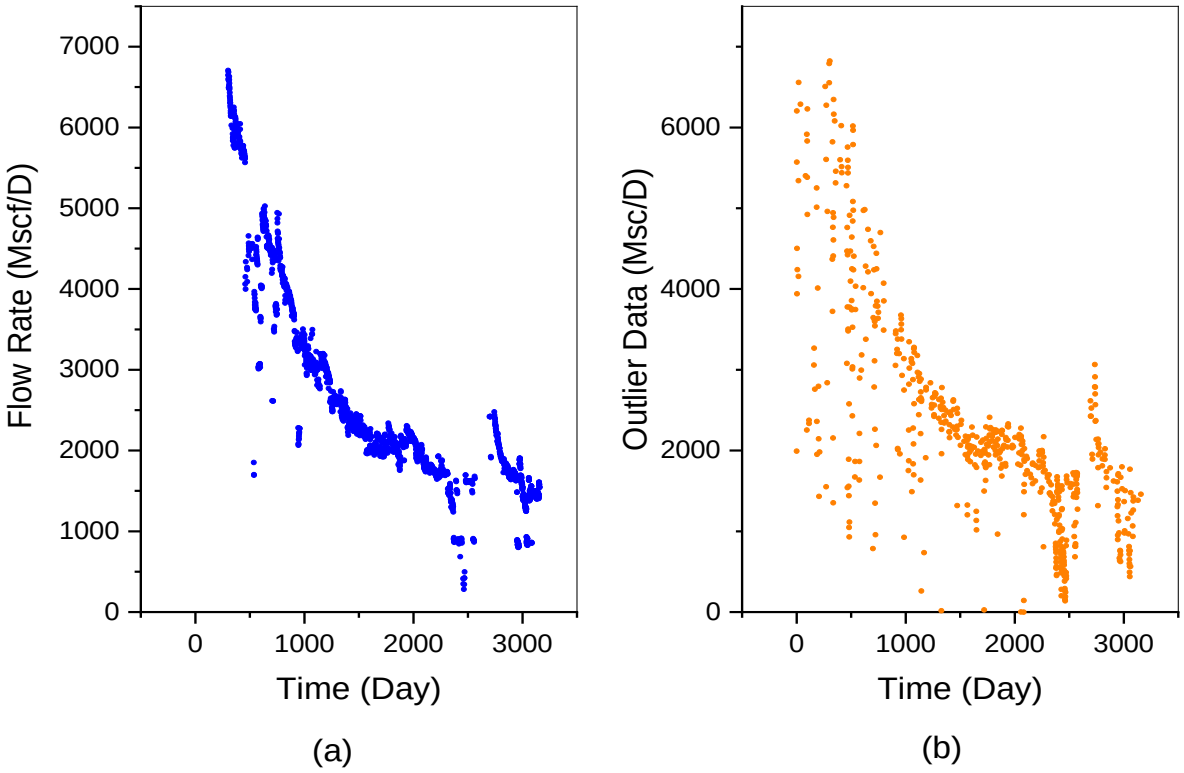

Figure 10. (a) The production data after removing 20% as outlier. (b) The removed data.

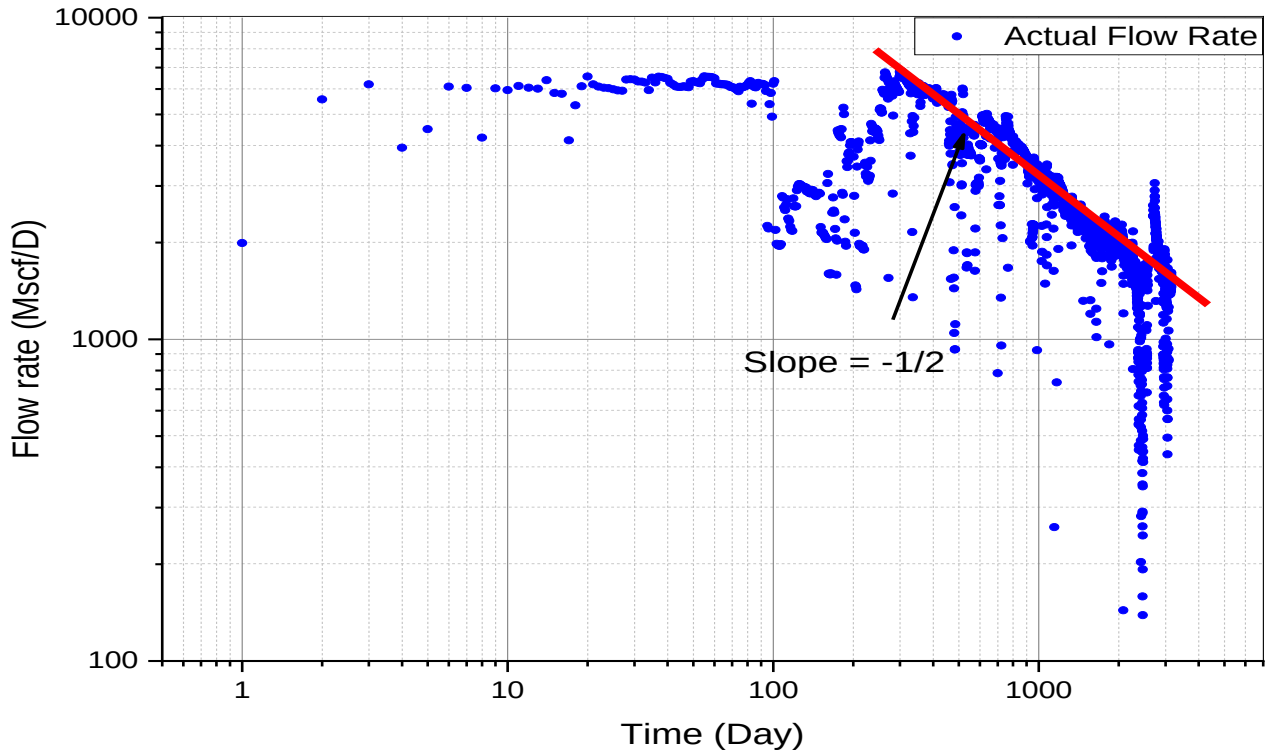

Figure 11. Shows identifying the flow regimes before removing the noise.

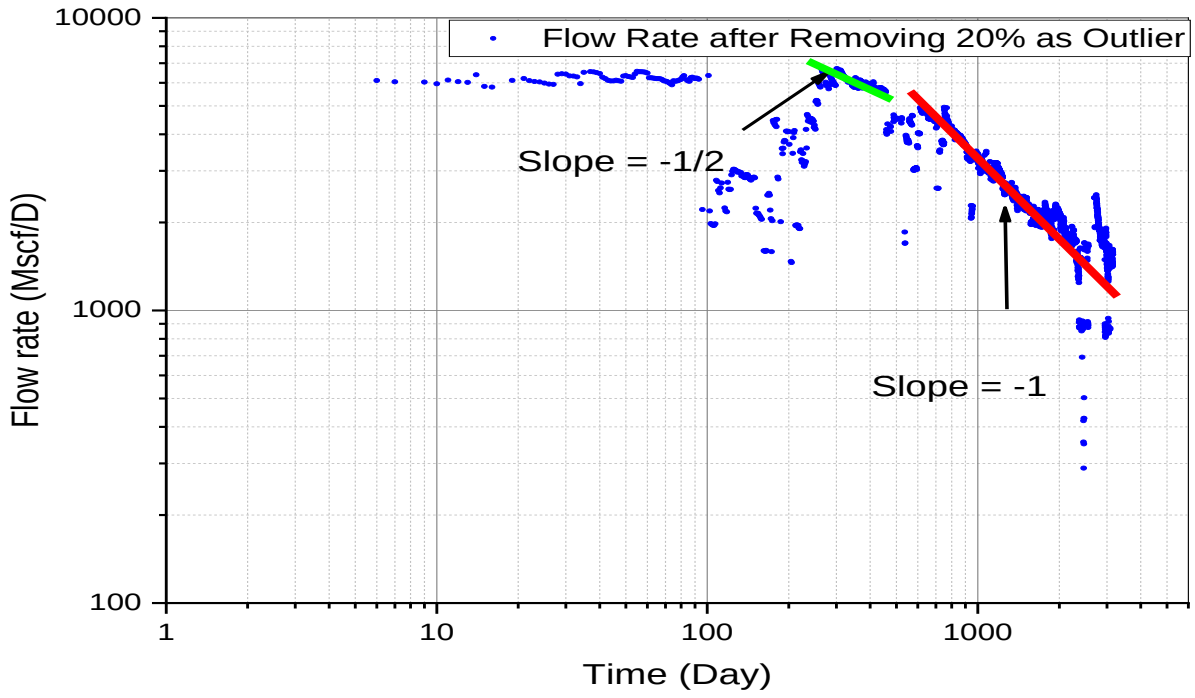

Figure 12. Shows identifying the flow regimes after removing 20% as the noise.

4.4. WELL_40

Figures (13) and (4.14) show the actual production profile, the production profile after removing 20% of the production data as noise and the removed noise of well_40 successfully.

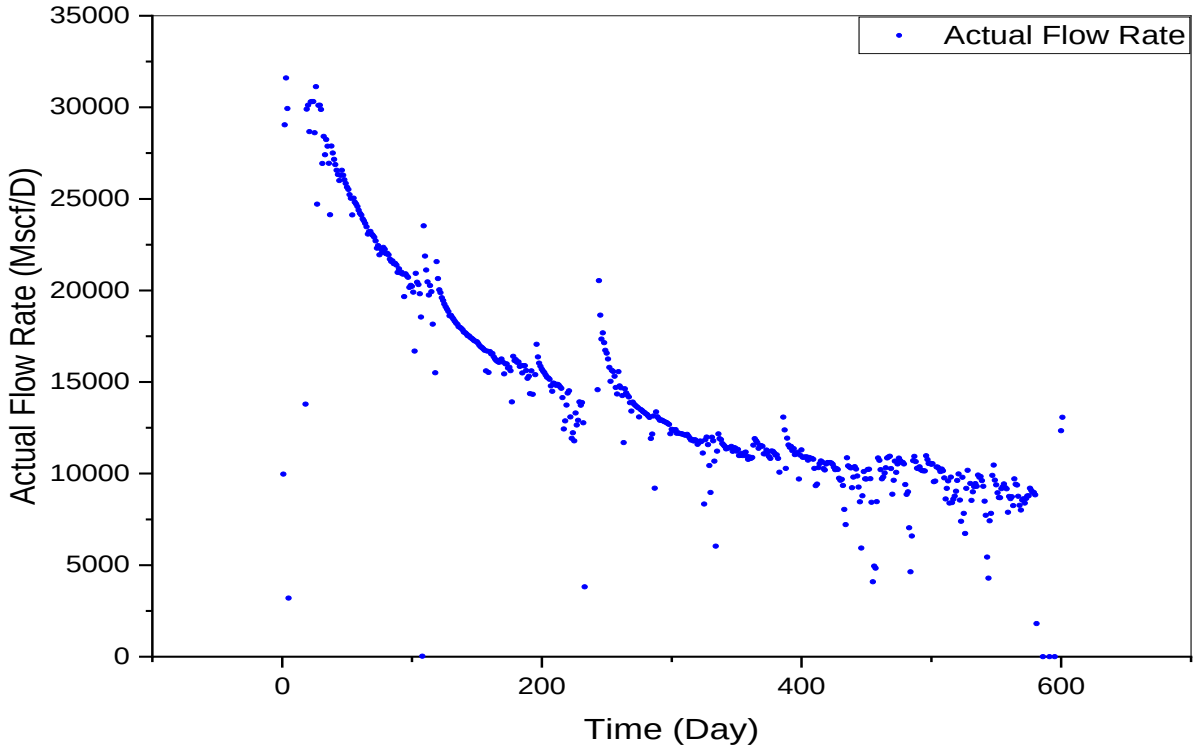

Figure 13. The actual production data before removing outlier.

Figures (15) and (16) show how the different flow regimes are identified from the log-log plot of the flow rate versus time by detecting the trend line with the characteristic slope of each one.

Looking at the production profile of this well, we could notice that it is too smooth especially at the early time of the production. Most of the noise was concentrated in the late time of the production profile.

The removed noise is scattered through all of the production profile. At the beginning, it removes the isolated points. After that, it removes closer by closer points without masking any trends within the production profile.

Figure (15) shows the log-log plot of the actual flow rate versus time before removing the outliers while **Figure (4.16)** shows the same plot but after removing 20% from the production data as noise successfully.

Before removing the noise, we identified two trend lines related to the bilinear and linear flow regimes as shown in **Figure (15).** After removing the noise, we identified three trend lines related to the bilinear, linear, and BDF as shown in **Figures (16).** Because most of the removed noise was from the early time of the production, we differentiated between the bilinear and linear flow regime clearly after removing the noise.

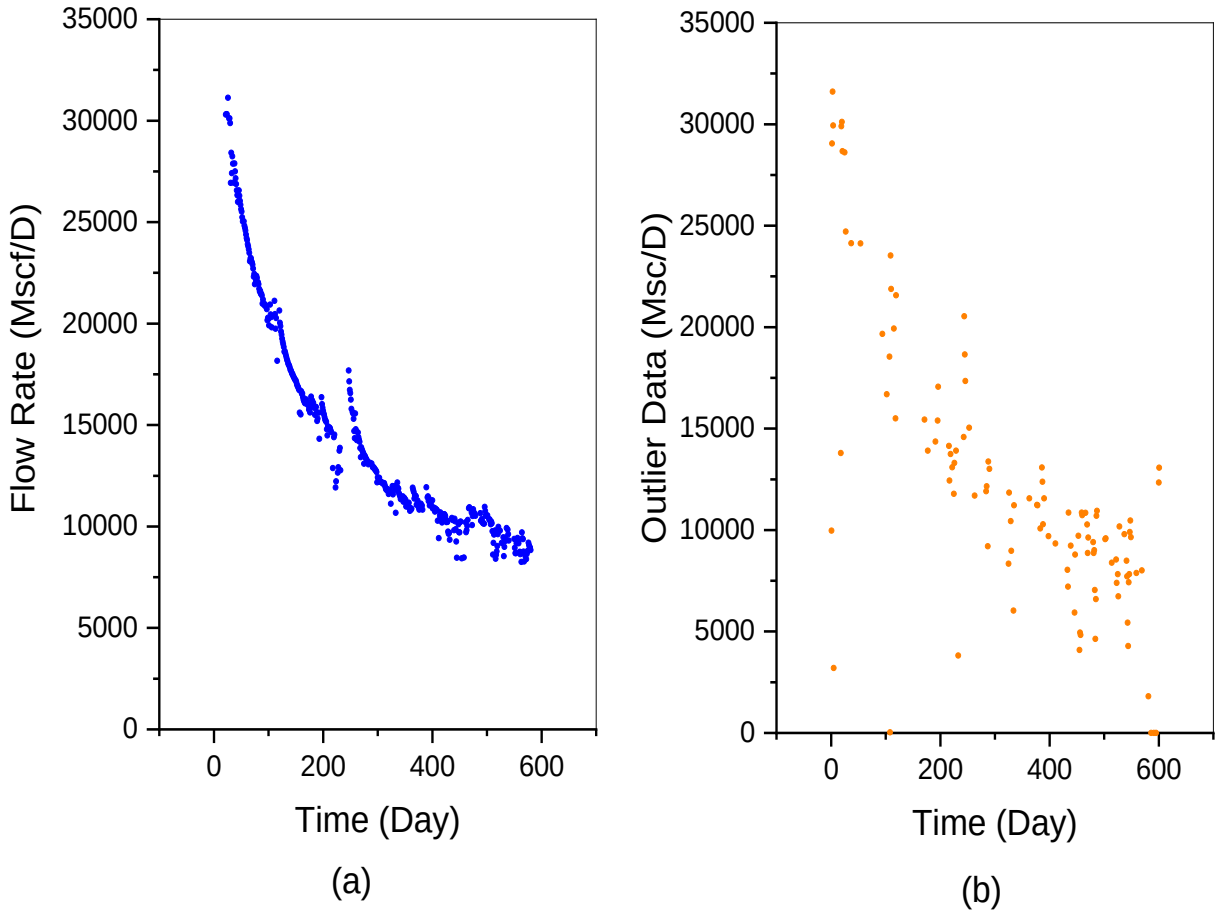

Figure 14. (a) The production data after removing 20% as outlier. (b) The removed data.

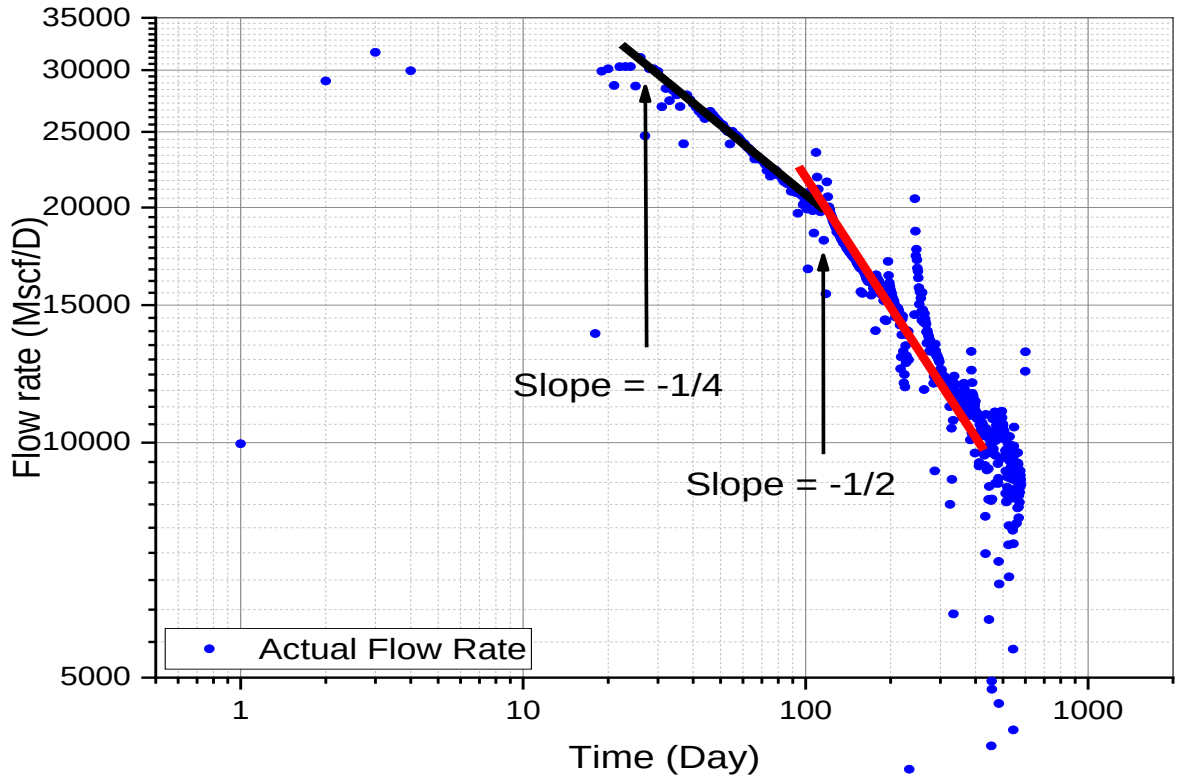

Figure 15. Shows identifying the flow regimes before removing the noise.

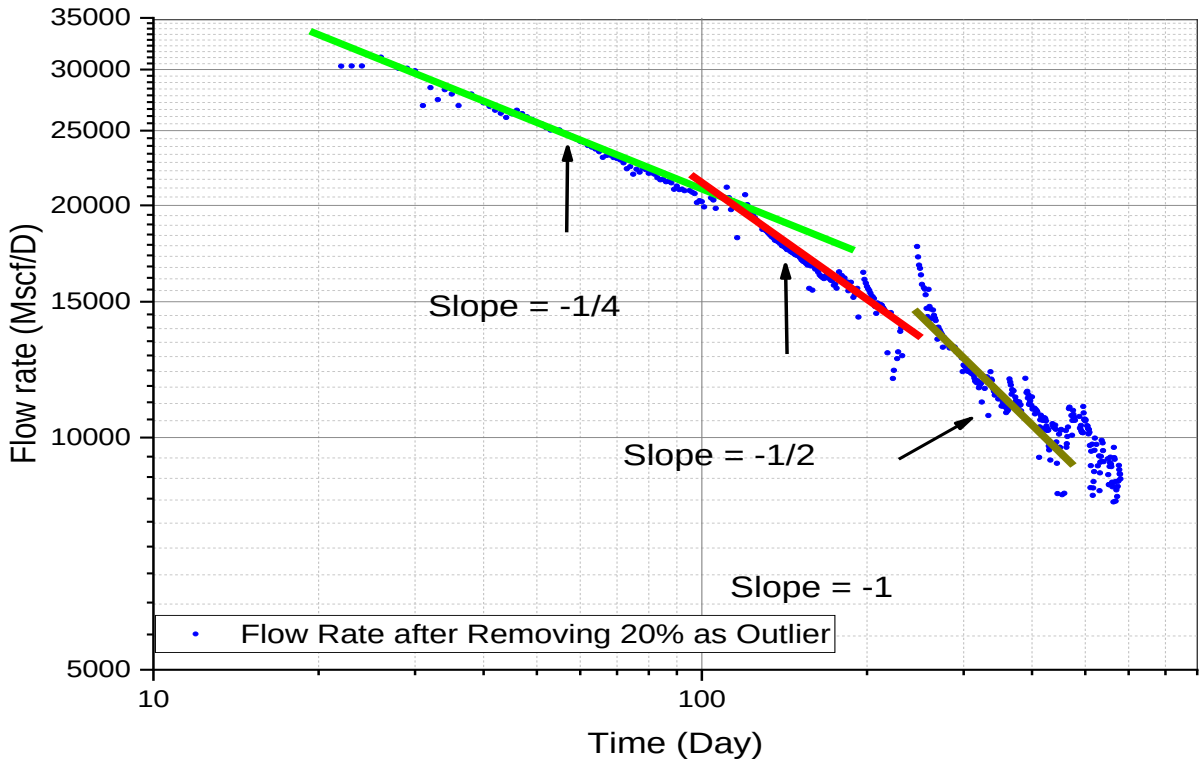

Figure 16. Shows identifying the flow regimes after removing 20% as the noise.

5. Conclusions and Recommendations

In this paper, we used the ABOD algorithm to improve the production data of the shale gas wells. This algorithm proved its efficiency in removing the noise and smoothing the production profile without any bias. Determining the different flow regimes related to the shale gas was effective and the trend line with the characteristics slope of each flow regime was much better and clear. Another advantage of the ABOD is that the production profile is improved based on the concentration of the noise. This means if the noise is spread all over the production profile, it will be removed equally and all the profile will be smoothed. Meanwhile, if the noise is concentrated in a certain part of the production profile while the other parts are smooth, the ABOD algorithm will focus only on the noisy part.

Acronyms

ABOD	=	Angle-based outlier detection
BDF	=	Boundary Dominated Flow
BHP	=	Bottom Hole Pressure
DCA	=	Decline Curve Analysis
EUR	=	Estimated Ultimate Recovery

References

[1] L. Zuo, W. Yu, K. Wu, A fractional decline curve analysis model for shale gas reservoirs, International Journal of Coal Geology. 163 (2016) 140–148. https://doi.org/10.1016/j.coal.2016.07.006.

[2] S. Huang, G. Ding, Y. Wu, H. Huang, X. Lan, J. Zhang, A semi-analytical model to evaluate productivity of shale gas wells with complex fracture networks, Journal of Natural Gas Science and Engineering. 50 (2018) 374–383. https://doi.org/10.1016/j.jngse.2017.09.010.

[3] R. Zhang, L. Zhang, H. Tang, S. Chen, Y. Zhao, J. Wu, K. Wang, A simulator for production prediction of multistage fractured horizontal well in shale gas reservoir considering complex fracture geometry, Journal of Natural Gas Science and Engineering. 67 (2019) 14–29. https://doi.org/10.1016/j.jngse.2019.04.011.

[4] B. Kulga, T. Ertekin, Numerical representation of multi-component gas flow in stimulated shale reservoirs, Journal of Natural Gas Science and Engineering. 56 (2018) 579–592. https://doi.org/10.1016/j.jngse.2018.06.023.

[5] O. Mahmoud, M. Ibrahim, C. Pieprzica, S. Larsen, EUR Prediction for Unconventional Reservoirs: State of the Art and Field Case, in: Day 3 Wed, June 27, 2018, SPE, Port of Spain, Trinidad and Tobago, 2018: p. D031S023R001. https://doi.org/10.2118/191160-MS.

[6] L. Ren, R. Lin, J. Zhao, V. Rasouli, J. Zhao, H. Yang, Stimulated reservoir volume estimation for shale gas fracturing: Mechanism and modeling approach, Journal of Petroleum Science and Engineering. 166 (2018) 290–304. https://doi.org/10.1016/j.petrol.2018.03.041.

[7] H. Yu, Y. Zhu, X. Jin, H. Liu, H. Wu, Multiscale simulations of shale gas transport in micro/nano-porous shale matrix considering pore structure influence, Journal of Natural Gas Science and Engineering. 64 (2019) 28–40. https://doi.org/10.1016/j.jngse.2019.01.016.

[8] Z. Liehui, S. Baochao, Z. Yulong, G. Zhaoli, Review of micro seepage mechanisms in shale gas reservoirs, International Journal of Heat and Mass Transfer. 139 (2019) 144–179. https://doi.org/10.1016/j.ijheatmasstransfer.2019.04.141.

[9] L. Germanou, M.T. Ho, Y. Zhang, L. Wu, Shale gas permeability upscaling from the pore-scale, Physics of Fluids. 32 (2020) 102012. https://doi.org/10.1063/5.0020082.

[10] Y. Meng, M. Li, X. Xiong, J. Liu, J. Zhang, J. Hua, Y. Zhang, Material balance equation of shale gas reservoir considering stress sensitivity and matrix shrinkage, Arabian Journal of Geosciences. 13 (2020) 1–9. https://doi.org/10.1007/s12517-020-05485-6.
[11] L. Chen, L. Zuo, Z. Jiang, S. Jiang, K. Liu, J. Tan, L. Zhang, Mechanisms of shale gas adsorption: Evidence from thermodynamics and kinetics study of methane adsorption on shale, Chemical Engineering Journal. 361 (2019) 559–570. https://doi.org/10.1016/j.cej.2018.11.185.
[12] Y. Cheng, W.J. Lee, D.A. McVay, Quantification of Uncertainty in Reserve Estimation From Decline Curve Analysis of Production Data for Unconventional Reservoirs, Journal of Energy Resources Technology. 130 (2008). https://doi.org/10.1115/1.3000096.
[13] M. Ibrahim, O. Mahmoud, C. Pieprzica, A New Look at Reserves Estimation of Unconventional Gas Reservoirs, in: OnePetro, 2018. https://doi.org/10.15530/URTEC-2018-2903130.
[14] T. Ahmed, Modern Decline Curve Analysis, in: Reservoir Engineering Handbook, Elsevier, 2019: pp. 1389–1461. https://doi.org/10.1016/B978-0-12-813649-2.00018-9.
[15] O. Mahmoud, S. Elnekhaily, G. Hegazy, Estimating Ultimate Recoveries of Unconventional Reservoirs: Knowledge Gained from the Developments Worldwide and Egyptian Challenges, International Journal of Industry and Sustainable Development. 1 (2020) 60–70. https://doi.org/10.21608/ijisd.2020.73505.
[16] M.H. Alqahtani, T. Ertekin, Shale Gas Reservoir Development Strategies using Complex Specified Bottom-hole Pressure Well Architectures, Sats. (2017). https://doi.org/10.2118/188144-ms.
[17] H. Zhang, E. Nelson, D. Olds, D. Rietz, W.J. Lee, Effective Applications of Extended Exponential Decline Curve Analysis to both Conventional and Unconventional Reservoirs, in: Day 3 Wed, September 28, 2016, SPE, Dubai, UAE, 2016: p. D031S039R007. https://doi.org/10.2118/181536-MS.
[18] L. Zuo, W. Yu, K. Wu, A fractional decline curve analysis model for shale gas reservoirs, International Journal of Coal Geology. 163 (2016) 140–148. https://doi.org/10.1016/j.coal.2016.07.006.
[19] W. Wang, D. Fan, G. Sheng, Z. Chen, Y. Su, A review of analytical and semi-analytical fluid flow models for ultra-tight hydrocarbon reservoirs, Fuel. 256 (2019) 115737. https://doi.org/10.1016/j.fuel.2019.115737.
[20] H. Shekhar Jha, H. Mustafa Ud Din Sheikh, W.J. Lee, Outlier Detection Techniques Help Us Identify and Remove Outliers in Production Data to Improve Production Forecasting, in: OnePetro, 2021. https://doi.org/10.15530/AP-URTEC-2021-208384.
[21] SPE Data Repository: Data Set: {1},Well Number: {12}, (n.d.). From URL: {https://www.spe.org/datasets/dataset_1/spreadsheets/dataset_1_well_12.xlsx}.
[22] SPE Data Repository: Data Set: {1},Well Number: {12}, (n.d.). From URL: {https://www.spe.org/datasets/dataset_1/spreadsheets/dataset_1_well_40.xlsx}.
[23] SPE Data Repository: Data Set: {1},Well Number: {12}, (n.d.). From URL: {https://www.spe.org/datasets/dataset_1/spreadsheets/dataset_1_well_35.xlsx}.
[24] SPE Data Repository: Data Set: {1},Well Number: {12}, (n.d.). From URL: {https://www.spe.org/datasets/dataset_1/spreadsheets/dataset_1_well_24.xlsx}.